Solution behavior of polyethylene oxide in water as a function of temperature and pressure

Stefan Bekiranov
Department of Physics, University of California, Santa Barbara, California 93106

Robijn Bruinsma
Department of Physics, University of California, Los Angeles, California 90077

Philip Pincus
Physics and Materials Departments, University of California, Santa Barbara, California 93106
(Received 8 May 1996)

A model of the solution behavior for hydrosoluble polymers [based on a model of Matsuyama and Tanaka, Phys. Rev. Lett. **65**, 341 (1990)] is introduced that accounts for hydrogen bonding of solvent molecules onto polymer chains. In the limit of small volume fraction of H-bonded solvent molecules, the resulting free energy has the standard Flory-Huggins form with a good solvent contribution to the effective χ parameter coming from the fraction of solvents H bonded to the chain. This simple theory is capable of semiquantitatively explaining the experimental temperature-concentration (T-ϕ) and temperature-pressure (T-P) phase diagrams of polyethylene oxide in water. [S1063-651X(96)04712-5]

PACS number(s): 64.70.Ja, 64.75.+g, 81.30.Dz, 82.30.Nr

I. INTRODUCTION

Understanding the behavior of hydrosoluble polymers is of biological and commercial interest [2–6]. There are generally two mechanisms by which hydrocarbon polymers become soluble in water: (i) attached polar groups on the polymers and (ii) hydrogen bonding between the chain and water; the latter is the subject of this paper. The most studied hydrosoluble polymer is polyethylene oxide (PEO) [7,8], which belongs to the polyepoxide group (general formula $[(CH_2)_nO]_x$, with $n=2$). Devanand and Selser's study of PEO in water [9] reveals an unusually large second osmotic virial coefficient A_2 and prefactor a in the scaling relation $R_g = aN^{0.58}$ [10], indicating that water is an extremely good solvent for PEO. The solubility of PEO in water is attributed to hydrogen bonding between water molecules and the oxygen on the polymer backbone.

A common feature in binary liquid mixtures that exhibit hydrogen bonding between the two components (e.g., nicotine plus water [11]) is closed-loop temperature-concentration phase boundaries [12]. The PEO temperature-concentration phase diagram exhibits these closed-loop phase boundaries [13–16] that are sensitive to the molecular weight of the chains. In fact, these closed loops shrink as a function of decreasing molecular weight to a point at $M_\eta \approx 2140$ [13].

Many polymers that are soluble in organic solvents have critical temperatures that are weakly sensitive to pressures up to 20 kbar [17]. In contrast, Cook, King, and Peiffer [18] found that increasing pressure ($\sim$4 kbar) dramatically lowers the lower critical solution temperature (LCST) of PEO in water to room temperature. Thus the picture that has emerged is that under ambient conditions, H bonding of water to the chain results in extremely good solvent properties. An increase of temperature or pressure decreases the solvent quality through the reduction of hydrogen bonds, thereby inducing phase separation.

Theoretical work [1,19,20] on this subject has been sparse compared to that of experiment. Below we present a brief review of the phenomenological models used to explain the behavior of hydrosoluble polymers and the open questions these works have generated.

Matsuyama and Tanaka (MT) [1] showed that formation of hydration complexes along the polymer chain produces a phase diagram that is consistent with the observed experimental phase diagram of PEO in water [13,21]. They assume that the solvent can stick (via H bonding) to the polymer, thereby defining a system of m clusters (i.e., m solvent molecules attached to a polymer) and free solvent. MT allow the number of attached solvents to *fluctuate* and treat each m cluster as a separate chemical species. Moreover, they explicitly assume that in the absence of H bonding the polymer is in a poor solvent (i.e., $\chi > 0.5$). They find that the good solvent quality of hydrosoluble polymers can be explained solely by the mechanism of binding the solvent to the chain. Furthermore, they show that the average number of attached solvents decreases with temperature, thereby exposing the polymer to a poor solvent at high enough temperatures. However, keeping track of the population of the various m clusters leads to a rather involved formalism in which the mixing free energy is not explicitly written as a function of the monomer volume fraction ϕ. Moreover, they do not address whether the solvent quality of hydrosoluble polymers is dominated by the average number of H-bonded solvents or whether fluctuation effects play a significant role.

Focusing on the formation of PEO aggregates [22] detected by light scattering [26], de Gennes [19] suggested that it might be possible to maintain the simplicity of the original Flory-Huggins theory for these materials. These aggregates are detected at temperatures below the LCST in a region of the T-ϕ plane where the measured second virial coefficient is positive (i.e., repulsive monomer-monomer interactions). de Gennes includes attractive *higher* virial coefficients to describe potential oligomer formation and goes on to show that

this leads to a novel phase separation below a temperature $\theta \sim 70$ °C, which is 30 °C below the LCST, where dilute *swollen* coils coexist with a dense polymer phase (i.e., aggregates). However, the microscopic mechanism by which higher negative virial coefficients are achieved is not discussed. We note that the model introduced by MT contains the feature that the good solvent quality depends on the fraction of H-bonded solvents, which decreases with increasing monomer concentration. Thus there may be a formal connection between de Gennes's theory and that of MT; however, this has not been explored.

In a previous work, we [20] studied the single-chain behavior of hydrosoluble polymers. We assumed that H bonding of water to monomer results in a good solvent contribution to the second virial coefficient $v_H(\phi,T,P)>0$. Furthermore, in a dense monomer environment, we assumed monomer-monomer contacts are capable of suppressing H bonding between the solvent and polymer. This leads to a concentration-dependent second virial coefficient where increasing the monomer concentration reduces solvent quality similar to de Gennes theory [19]. Adding $v_H(\phi,T,P)$ to the Flory single-chain free energy leads to a barrier between the swollen and collapsed states, while the standard Flory free energy has only a single minimum. By simply expanding $v_H(\phi,T,P)$ to linear order in pressure P, our single-chain theory captured the experimental R_η versus the pressure curve well for PEO in water [18]. However, the molecular weight dependence of the experimental critical pressure could not be explained by this theory.

In this work, we start with a free energy that allows for attachment of solvent molecules onto polymer chains via hydrogen bonding. We derive the distribution of chains with m attached solvents and show that the fluctuations in the fraction of attached solvents are $\sim 1/\sqrt{N}$, where N is the number of monomers on a chain. For typical polymers, $1/\sqrt{N}$ is small. We use this fact to arrive at a mean-field model in which we assume that all polymers have the *same* number of attached solvents $\overline{m}$. We explicitly are able to write the free energy as a function of monomer concentration and find that it is well approximated by the Flory-Huggins form in the neighborhood of the coexistence curve. Furthermore, we show that higher virial coefficients are all *positive*; hence our model does not describe aggregate formation. Moreover, we introduce a model for the pressure dependence of $\overline{m}$ based on the idea of a preferred H-bonding volume [27]. We go on to show that our generalized Flory-Huggins free energy is capable of explaining the experimental T-P-ϕ phase diagram of PEO in water. More specifically, our simple model (i) fits the experimental critical temperature versus M_w data well, including the double critical point at $M_w \sim 2140$, (ii) semiquantitatively captures the experimental T-ϕ coexistence curves, (iii) fits the P-T phase diagram to within experimental error, and (iv) semiquantitatively agrees with the cloud point pressure versus M_w curve. Finally, our theory predicts reentrant behavior in the P-T phase diagram, which has recently been observed in the poly(N-vinyl-2-pyrrolidone) in water system [28].

II. GENERALIZED FLORY-HUGGINS FREE ENERGY

Assuming we have a solution of m clusters (i.e., a polymer and m attached solvents) with volume fraction ϕ_{m+1} and free solvent with volume fraction ϕ_0, the mixing free energy per site is

$$\frac{F}{T}=\sum_{m=0}^{N}\frac{\phi_{m+1}}{N+m}\ln\phi_{m+1}+\phi_0\ln\phi_0 + \sum_{m=0}^{N}\frac{\phi_{m+1}}{N+m}\left[m\frac{\Delta F_0}{T}-\ln\frac{f!}{(f-m)!m!}\right]+\chi\phi(1-\phi). \tag{1}$$

The first two terms constitute the contribution to the entropy of mixing coming from the translational degrees of freedom of m clusters and a free solvent. The third term constitutes the free-energy change due to forming m clusters, where $\Delta F_0=\Delta\mathcal{E}_0-T\Delta S_0$ is the free-energy difference between a bound and free solvent and $\ln[f!/(f-m)!m!]$ is the entropy arising from the number of unique configurations that m attached solvents can assume on a chain with f bonding sites. For simplicity, we assume that each monomer unit is capable of forming only one hydrogen bond (i.e., $f=N$ at $P=0$ [29]). The last term is the ''bare'' monomer solvent interaction with a *poor solvent* χ (>0.5) parameter, which accounts for the hard-core, van der Waals, and ''hydrophobic'' interactions. In the temperature range of interest, we simply assume $\chi(T)=A-BT$. Finally, the incompressibility condition for this system is given by

$$\sum_{m=0}^{N}\phi_{m+1}+\phi_0=1. \tag{2}$$

We find the distribution of m clusters by minimizing (1) with respect to ϕ_{m+1} subject to the constraint

$$\sum_{m=0}^{N}\phi_{m+1}\frac{N}{N+m}=\phi, \tag{3}$$

where ϕ is the volume fraction of monomers. We find

$$\frac{c_{m+1}}{c_1}=\exp\left[m\left(\ln\phi_0+1-\frac{\Delta F_0}{T}\right)+f\ln f-m\ln m -(f-m)\ln(f-m)\right], \tag{4}$$

where $c_{m+1}=\phi_{m+1}/(N+m)$ is the concentration of chains with m attached solvents. As a function of m, c_{m+1} is well approximated by a Gaussian peaked at

$$\frac{\overline{m}}{f}=\frac{\lambda(T)\phi_0}{\lambda(T)\phi_0+1}, \tag{5}$$

where $\lambda(T)\equiv\exp[1-\Delta F_0/T]$, of width

$$\frac{\Delta m}{f}=\sqrt{\frac{1}{f}\left(\frac{\overline{m}}{f}\right)\left(1-\frac{\overline{m}}{f}\right)}\quad . \tag{6}$$

From (6), we see that $\Delta m/\overline{m}=\sqrt{(1/\overline{m})(1-\overline{m}/f)}$. Unless the temperature is extremely high or the volume fraction of solvent very low, $\overline{m}\sim f=N$ and $\Delta m/\overline{m}\sim 1/\sqrt{N}$. For typical polymers, $1/N\ll 1$; thus fluctuations in the number of H-bonded solvents is negligible and the distribution shown in (4) is sharply peaked at $\overline{m}$.

We note that Eq. (1) resembles the free energy of living polymers [30]. In the case of living polymers, the size distribution of aggregates is usually an *exponential* function of the number of aggregating molecules, whereas, in our case, we find a sharply peaked Gaussian. The essential difference between living and hydrosoluble polymers is that the *backbone* of the hydrosoluble polymers acts as a source of $\sim N$ bonding sites and gives rise to a mixing entropy of bonded and unbonded sites along the chain. This ''bond'' entropy, which is given by the last three terms within the exponential of Eq. (4), is sharply peaked for large N at $m^*=N/2$, where the number of configurations is maximum. The competition between the local free energy change due to bond formation and the bond entropy simply shifts this sharp peak from m^* to $\overline{m}$. We will now use the fact that the fluctuations are insignificant and simplify (1) by assuming *every* polymer has the *same* number of bound solvents $\overline{m}$.

The mixing free energy per site for a solution with $\overline{m}$ clusters, (i.e., *every* polymer having exactly $\overline{m}$ attached solvents) and a free solvent molecules is (neglecting terms linear in ϕ)

$$\frac{F}{T}=\frac{\phi_{\overline{m}+1}}{N+\overline{m}}\ln\frac{\phi_{\overline{m}+1}}{N+\overline{m}}+\phi_0\ln\phi_0+\frac{\phi_{\overline{m}+1}}{N+\overline{m}}\left[\overline{m}\,\frac{\Delta F_0}{T}-\ln\frac{f!}{(f-\overline{m})!\,\overline{m}!}\right]+\chi\phi(1-\phi). \tag{7}$$

Because the number of chains trivially equals the number of polymers with $\overline{m}$ bound solvents, (3) simplifies to

$$\frac{\phi_{\overline{m}+1}}{N+\overline{m}}=\frac{\phi}{N}. \tag{8}$$

Furthermore, the incompressibility condition Eq. (2) becomes

$$\phi_0=1-\phi_{\overline{m}+1}=1-\left(1+\frac{\overline{m}}{N}\right)\phi, \tag{9}$$

where $(\overline{m}/N)\phi$ is the volume fraction of bound solvent.

Minimizing F [Eq. (7)] with respect to $\overline{m}$, we recover the result for the average equilibrium number of bound solvents $\overline{m}/f$, shown in Eq. (5), which we rewrite as

$$\ln\phi_0+1+\ln\left(\frac{f}{\overline{m}}-1\right)-\frac{\Delta F_0}{T}=0. \tag{10}$$

We see that the equilibrium number of bound solvents is determined by balancing the loss in bulk translational entropy, the gain in configurational entropy along the chain, and the change in the local free energy of the solvent molecule due to bond formation. We may simplify Eq. (7) by using Eqs. (8)–(10) to arrive at the final form of the mean-field free energy (without additional approximations)

$$\frac{F}{T}=\frac{\phi}{N}\ln\phi+(1-\phi)\ln(1-\phi)+\chi\phi(1-\phi)+(1-\phi)\ln\left(1-\frac{\overline{m}}{N}\,\phi\,\frac{1}{1-\phi}\right)+\frac{f}{N}\,\phi\,\ln\left(\frac{f}{N}-\frac{\overline{m}}{N}\right)+\frac{\overline{m}}{N}\,\phi. \tag{11}$$

The first three terms constitute the standard Flory-Huggins free energy [31] for a polymer in poor solvent. The last three terms are the good solvent contribution to the free energy due to the volume fraction of solvent $(\overline{m}/N)\phi$ being H bonded to the polymer.

We may express $\overline{m}/N$ and, thereby, F explicitly as functions of temperature and volume fraction of monomer by combining Eqs. (9) and (10):

$$\frac{\overline{m}}{N}=\frac{C(\phi)-\sqrt{C(\phi)^2-4\mathcal{L}(T)^2\,\frac{f}{N}\,\phi(1-\phi)}}{2\mathcal{L}(T)\phi}, \tag{12}$$

where

$$C(\phi)=1+\mathcal{L}(T)\left(\frac{f}{N}-1\right)\phi, \tag{13}$$

$$\mathcal{L}(T)\equiv\frac{\lambda(T)}{\lambda(T)+1}, \tag{14}$$

and

$$\lambda(T)=\exp\left[r\left(\frac{T_m}{T}-1\right)\right], \tag{15}$$

which is equivalent to the expression found by MT [1]. We have reparametrized the statistical weight for forming a H bond along the chain $\lambda(T)$. In particular, we have introduced the parameter T_m, which is defined by $\mathcal{L}(T_m)\equiv\frac{1}{2}$. From Eqs. (12) and (13), we see that for $\phi\to 0$ (i.e., dilute limit), $\overline{m}/N\to\mathcal{L}(T)$. Thus, similar to the definition of the helix-coil transition [32] in which the helix is defined to ''melt'' when the fraction of helical segments is equal to $\frac{1}{2}$, we define a ''melting'' temperature T_m where the fraction of attached solvents (for an isolated coil) is reduced to $\frac{1}{2}$. We may write T_m in terms of the energy difference $\Delta\mathcal{E}_0$ and entropy difference ΔS_0 between a bound and unbound solvent [33] as $\Delta\mathcal{E}_0=T_m(\Delta S_0+1)$. Finally, r is defined by the ratio $r\equiv-\Delta\mathcal{E}_0/T_m$. Equations (11) and (12) constitute a mean-field solution theory of polymers that associate with a solvent where fluctuations in the fraction of attached solvent have been neglected.

Using Eqs. (11) and (12) (with $f=N$), we may expand the free energy in small ϕ, giving

$$\frac{F}{T}\approx\frac{\phi}{N}\ln\phi+\tfrac{1}{2}v\phi^2+\tfrac{1}{6}w\phi^3+\tfrac{1}{24}u\phi^4+\cdots, \tag{16}$$

where the second [34], third, and fourth virial coefficients are given by

$$v=1-2\chi+\mathcal{L}(2+\mathcal{L}), \tag{17}$$

$$w=1+\mathcal{L}^3(4+3\mathcal{L}), \tag{18}$$

and

$$u=2+\mathcal{L}^3(-8-6\mathcal{L}+24\mathcal{L}^2+20\mathcal{L}^3), \tag{19}$$

respectively. In this work, we will be interested in understanding the experimental T-ϕ phase diagram of PEO in water [13–16]. As mentioned above, χ is the bare poor solvent interaction parameter; thus, from Eq. (17) we see that the good solvent contribution to the second virial coefficient comes from the third term $\mathcal{L}(2+\mathcal{L})$. Within the context of our theory, we expect the polymer to be in a poor solvent around $T\sim T_m$, namely, when the fraction of H bonds begin to melt off the chain [35]. Indeed, MT find $T_m\approx 398$ ° K for PEO in water, which is around the LCST of this system. Thus we expect $\mathcal{L}(T)\lesssim\frac{1}{2}$ in the neighborhood of the coexistence curve and the contribution of H bonding on all virial coefficients beyond second order to be small. At high temperatures (i.e., $T\gtrsim T_m$), the free energy [Eq. (11)], is well approximated by

$$\frac{F}{T}\approx\frac{\phi}{N}\ln\phi+(1-\phi)\ln(1-\phi)+\left[\chi(T)-\mathcal{L}(T)\left(1+\frac{\mathcal{L}(T)}{2}\right)\right]\phi(1-\phi), \tag{20}$$

which is exactly of the Flory-Huggins form with an effective χ parameter containing the bare poor solvent χ plus a good solvent contribution coming from the fraction of H bonds formed along the chain.

A simple physical interpretation of the effect of H bonding solvent molecules onto the chain is found by retaining the dominant contributions to the free energy in $\overline{m}/N$ and $\mathcal{L}(T)$. To lowest order in $\overline{m}/N$, Eq. (11) is approximated by (with $f=N$)

$$\frac{F}{T}\approx\frac{\phi}{N}\ln\phi+(1-\phi)\ln(1-\phi)+\chi\phi(1-\phi)-\frac{\overline{m}}{N}\phi. \tag{21}$$

To lowest order in $\mathcal{L}(T)$, Eq. (12) is given by

$$\frac{\overline{m}}{N}\approx\mathcal{L}(T)(1-\phi). \tag{22}$$

Thus the free energy of the system is simply given by the usual Flory-Huggins expression minus k_BT per bound solvent molecule and the fraction of attached solvent assumes the form of a simple Langmuir isotherm as a function of temperature. This resembles the physics of simple adsorbing surfaces [30], where polymer in this case acts as the effective surface.

III. EFFECT OF PRESSURE ON HYDROGEN BONDING

Finally, we will also be interested in understanding the experimental T-P phase diagram of PEO in water [18]. To understand the effect of pressure on the H bonds formed along the chain, we use a simple, phenomenological model of water introduced by Poole *et al.* [27]. They assume that H bonds have a preferred length, which leads to a preferred volume for the formation of H bonds, V_{HB}. The application of pressure ($V<V_{\mathrm{HB}}$) or tension ($V>V_{\mathrm{HB}}$) introduces a *global* geometric constraint, which does not allow all H bonds to form at the preferred volume, thereby suppressing H bonding. For $V\neq V_{\mathrm{HB}}$, they assume only a fraction f' of the total bonds form at the optimal local H-bonding volume and $1-f'$ are found at an unfavorable volume (i.e., ''broken bonds''). They assume that f' is given by

$$f'=\exp\left\{-\left[\frac{(V-V_{\mathrm{HB}})}{\sigma'}\right]^2\right\}, \tag{23}$$

where σ' characterizes the width in V beyond which only a small number of H bonds are found at the optimum local volume.

In the case of hydrosoluble polymers, we assume that the water molecules that are H bonded to the chain are also H bonded to the rest of the water network. Kjellander and Florin [36] argued that the solubility of PEO in water is due to the oxygen-oxygen spacing along the chain providing a good structural fit to the water H-bonding network. We assume that application of pressure or tension introduces a global geometric constraint that both suppresses the fraction of water-water H bonds and frustrates the good structural fit between PEO and the water network. This leads to a reduction of the effective number of bonding sites f. For $V\neq V_{\mathrm{HB}}$, we assume that the effective number of bonding sites is given by an expression similar to (23),

$$\frac{f}{N}=\exp\left\{-\left[\frac{(V-V_{\mathrm{HB}})}{\sigma}\right]^2\right\}, \tag{24}$$

where $\sigma\neq\sigma'$ in general.

We find the dependence of f/N on pressure by using the equation of state of the system

$$V-V_{\mathrm{HB}}\approx -PK_TV_{\mathrm{HB}}, \tag{25}$$

where $K_T\equiv-(1/V)(\partial V/\partial P)_T$ is the system's isothermal compressibility. Using (24) and (25), we find

$$\frac{f}{N}=\exp\left\{-\left[\frac{PK_TV_{\mathrm{HB}}}{\sigma}\right]^2\right\}, \tag{26}$$

which we assume is well approximated by

$$\frac{f}{N}\approx 1-\gamma P^2, \tag{27}$$

where

$$\gamma=\left(\frac{K_T V_{\mathrm{HB}}}{\sigma}\right)^2, \tag{28}$$

for pressures reaching ~5 kbar (i.e., pressure scale of experiments [18]).

Finally, we are able to find the pressure dependence of $\overline{m}/N$ and the free energy of mixing by using Eqs. (11), (12), and (27). The fraction of H bonds on the polymer is given by

$$\frac{\overline{m}}{N}=\frac{1-\mathcal{L}\phi\gamma P^2-\sqrt{(1-\mathcal{L}\phi\gamma P^2)^2-4\mathcal{L}^2\phi(1-\phi)(1-\gamma P^2)}}{2\mathcal{L}\phi}. \tag{29}$$

Because the experimental T-P phase diagram was measured at dilute polymer concentrations, we may expand the free energy in small ϕ as in Eq. (16). Keeping only the contributions to second order in ϕ arising from H bonding, we find that the mixing free energy is given by

$$\frac{F}{T}\approx\frac{\phi}{N}\ln\phi+(1-\phi)\ln(1-\phi)+\chi_{\mathrm{eff}}(T,P)\phi(1-\phi), \tag{30}$$

where

$$\chi_{\mathrm{eff}}(T,P)\equiv\chi(T)-\mathcal{L}(T)(1-\gamma P^2)\left(1+\frac{\mathcal{L}(T)(1-\gamma P^2)}{2}\right). \tag{31}$$

We will now show that by using Eqs. (30) and (31) we are able to explain the experimental phase diagrams of PEO in water.

IV. COMPARISON OF THEORY TO EXPERIMENTAL PHASE DIAGRAMS

We investigate whether our simple model is capable of explaining the experimental T-P-ϕ phase diagram of PEO in water as a function of molecular weight. We begin by fitting the measured critical temperature T_c [both LCST and upper critical solution temperature (UCST)] versus molecular weight with four parameters A, B, r, and T_m with the constraint that r and T_m take values that are consistent with known H-bonding energies and melting temperatures. With one additional parameter γ, we fit the experimental cloud point pressure versus temperature phase diagram. We show that the resulting theoretical T-ϕ, P-M_w, and P-ϕ phase diagrams are in reasonable agreement with that of experiment.

We begin with the closed-loop T-ϕ phase diagram. The existence of a closed-loop miscibility gap has a simple physical explanation [37]. At ambient temperatures, H bonding of a solvent onto a polymer leads to a mixed phase. Increasing temperature near the boiling point of water where H bonds begin to break exposes the polymer to poor solvent and gives rise to a two-phase region. Increasing temperature further favors entropy of mixing and the system returns to a mixed phase.

For PEO in water, these close loops shrink with decreasing molecular weight down to a point at M_η~2140 (i.e., N~48.6) [13], where the polymer is soluble at all temperatures and concentrations. To see if this sensitivity to molecular weight can be accounted for solely by the translational entropy of the chains (which is the only N-dependent quantity in the theory), we fit the critical temperature T_c (both LCST and UCST) versus number of monomers N with

$$\chi(T_c)-\mathcal{L}(T_c)\left(1+\frac{\mathcal{L}(T_c)}{2}\right)=\frac{1}{2}+\frac{1}{\sqrt{N}}. \tag{32}$$

The results are shown in Fig. 1. The open squares are experimental data taken from Saeki *et al.* [13] and the solid squares are from Bae *et al.* [14]. In the region of T_c~400 K, the Saeki *et al.* and Bae *et al.* data appear to disagree. If we ignore the three Saeki *et al.* points in this neighborhood, we get a rather good fit and the collapse of the closed loops at $N=48.9$ and $T_c=478$ K. Although we are able to achieve reasonable fits of the Saeki *et al.* data alone, they are not nearly as good as presented in Fig. 1. We find that r and T_m take the values $r=5.38$ and $T_m=447.6$ K, which correspond to $\Delta\mathcal{E}_0\sim-8kT_{\mathrm{room}}$. We expect the order of magnitude of $\Delta\mathcal{E}_0$ to be that of the water-water H bond ϵ_{HB} [33]. Indeed, in their model of pure water, Poole *et al.* [27] find

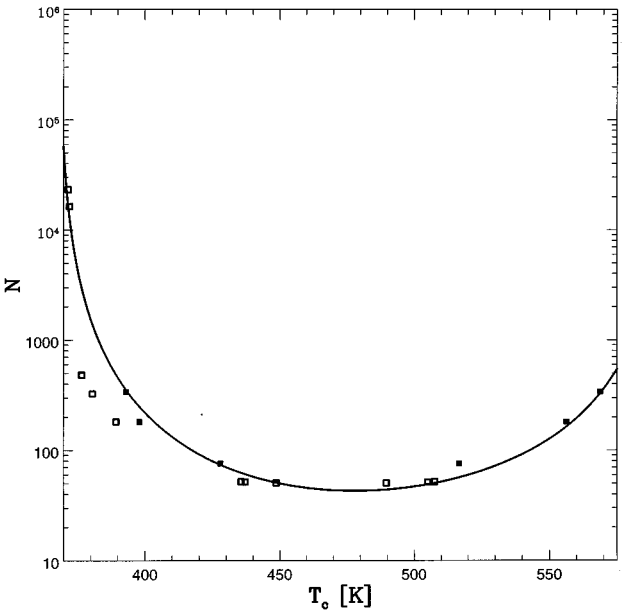

FIG. 1. Critical temperature T_c vs the number of monomer units N on a PEO chain. Open squares are the experimental data of Saeki *et al.* [13] and solid squares are the data of Bae *et al.* [14]. The solid line is the fitted theoretical curve using Eq. (32).

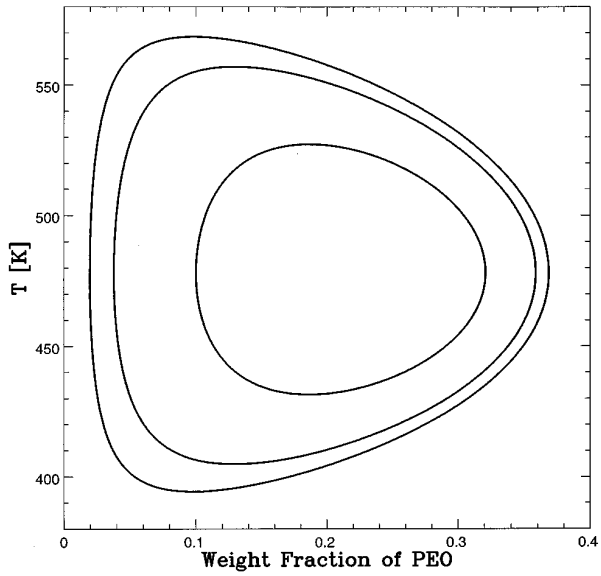

FIG. 2. Temperature-weight fraction spinodal, calculated from Eq. (33) for $M_w=3350$, 8000, and 15 000 PEO, which correspond to the inner, middle, and outer curves, respectively.

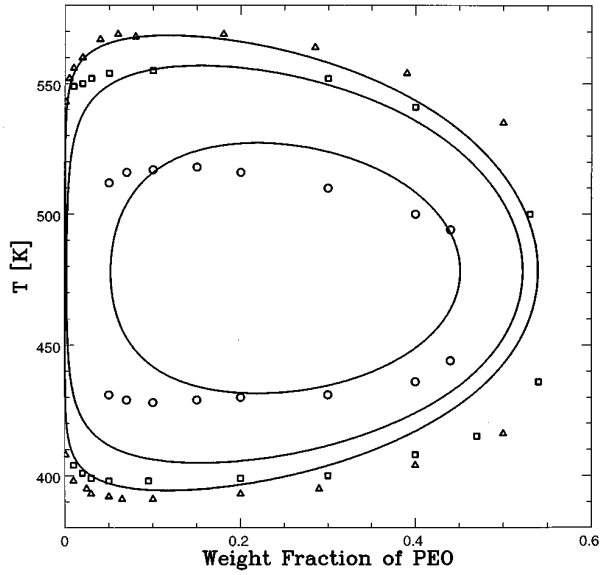

FIG. 3. Temperature-weight fraction coexistence curve for $M_w=3350$, 8000, and 15 000 PEO. Circles, squares, and triangles are the experimental cloud points of Bae *et al.* [14] for $M_w=3.35$, 8.0, and 15.0×10^3, respectively. Solid lines are the corresponding calculated coexistence curves.

$\epsilon_{\mathrm{HB}}\sim-8.8kT_{\mathrm{room}}$. The remaining parameters that determine χ are $A=2.884\,57$ and $B=0.003\,62$.

Using the parameters obtained from the fit, we compare the theoretical temperature weight fraction phase diagrams to that of Bae *et al.* [14]. In Fig. 2 we first show the calculated spinodals (i.e., $\partial^2F/\partial\phi^2=0$) given by

$$2\left[\chi(T)-\mathcal{L}(T)\left(1+\frac{\mathcal{L}(T)}{2}\right)\right]=\frac{1}{N\phi}+\frac{1}{1-\phi} \tag{33}$$

and we obtain the weight fraction of polymer, w from ϕ using the relation

$$w\approx\frac{44\phi}{18(1-\phi)+44\phi}, \tag{34}$$

where the molecular weight of a monomer is 44 and that of water is 18. In Fig. 3 we show the theoretical coexistence curve found by equating the chemical potential and osmotic pressure in the two phases [i.e., $\mu(\phi')=\mu(\phi'')$ and $\Pi(\phi')=\Pi(\phi'')$ [31]] along with the corresponding experimental cloud points of Bae *et al.* [14]. We note that the only input from the fitting are the approximate values of the LCST and the UCST for a given M_w; thus a test of the theory is how well the resulting theoretical phase diagram compares with that of experiment. The experimental coexistence curves extend beyond that of the theory into higher polymer concentrations, indicating that at higher concentrations PEO is in a poorer solvent than our lowest-order free energy Eq. (30) predicts. Within the context of our model, this may be remedied by retaining higher-order terms in the expansions shown in Eq. (16). Nevertheless, the agreement between theory and experiment is reasonable [38].

Starting at ambient pressure, the LCST of dilute PEO with $M_w=270\,000$ in water is 373 K. Cook, King, and Peiffer [18] found that application of pressure increased the LCST slightly up to 2 kbar and increasing pressure further dramatically reduces the LCST to room temperature at $P_t\sim4.3$ kbar (see Fig. 4). Furthermore, they find that at *fixed* concentration the cloud point pressure (with $T=295.65$ K) increases with decreasing N as $1/\sqrt{N}$ (see Fig. 5). They attributed this N dependence to the critical point behavior of Flory-Huggins theory where

$$\chi_c=\frac{1}{2}+\frac{1}{\sqrt{N}}. \tag{35}$$

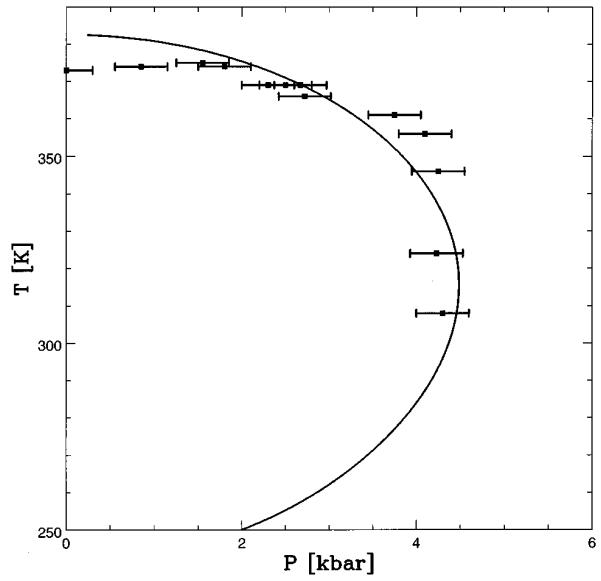

FIG. 4. Spinodal pressure vs temperature, calculated from Eq. (36) for $M_w=270\,000$ PEO at $\phi=0.002\,77$. Solid squares are the experimental cloud point data of Cook, King, and Peiffer [18].

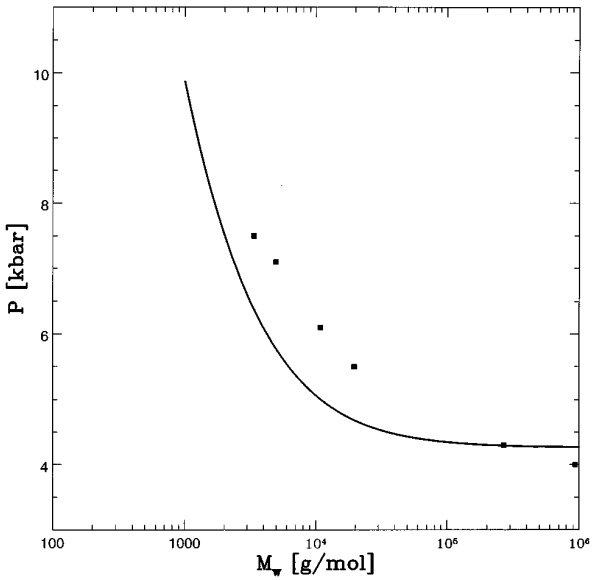

FIG. 5. Spinodal pressure vs molecular weight of PEO, calculated from Eq. (36) at $T=295.65$ K and $\phi=0.0554$. Solid squares are the experimental cloud point data of Cook, King, and Peiffer [18].

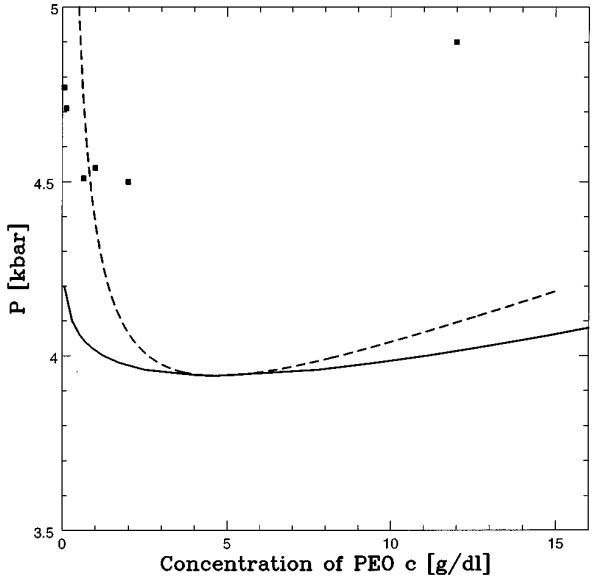

FIG. 6. Spinodal pressure (dashed curve) and binodal pressure (solid curve) vs concentration of polymer calculated for $M_w=252\,000$ PEO at $T=298.15$ K. Solid squares are experimental cloud point data of Sun and King [44].

However, the concentration was fixed in the experiment while the validity of Eq. (35) requires one to remain at the critical concentration ϕ_c, which varies with molecular weight as $1/\sqrt{N}$.

Within the context of our simple model, the N dependence of the cloud point pressure is due to the translational entropy of the chains. From (30), we find the spinodal pressure for dilute solution of polymer is given by

$$P=\sqrt{\frac{1}{\gamma\mathcal{L}(T)}\left[\mathcal{L}(T)+1-\sqrt{1+2\chi(T)-\left(\frac{1}{N\phi}+\frac{1}{1-\phi}\right)}\right]}. \tag{36}$$

For simplicity, we use Eq. (36) to investigate how well our theory compares to the experimental results of Cook, King, and Peiffer [18]. We set $\gamma=0.003$ bar^{-2}, which gives the best fit of the experimental P-T phase diagram shown in Fig. 4 for $M_w=270\,000$ at $c=1$ g/dl of PEO in water (i.e., $\phi\sim0.003$ in our case). We find that the theoretical curve qualitatively captures the dramatic drop in the LCST as $P\rightarrow4$–5 kbar and shows good semiquantitative agreement with the experimental curve. However, the slow rise in the LCST from ambient pressure up to 2 kbar is not captured. In typical polymer systems, the LCST gradually increases with pressure, an effect that has been theoretically predicted and experimentally observed [39–43]. In this work, we have neglected these effects and focused on the dominant effect pressure has on hydrogen bonding between PEO and water.

In Fig. 5, we plot the spinodal pressure versus molecular weight of PEO chains at $T=295.65$ K and concentration $c=20$ g/dl (i.e., $\phi\sim0.06$). Although the fit is reasonable, the experimental cloud point varies from ~4 to ~7.5 kbar, while the theoretical spinodal varies from ~4.3 to ~6.5 kbar across the full M_w range. The fact that the experimental cloud point appears to be more sensitive to M_w than that of theory may be due to our truncating f/N to second order in P, which is a poor approximation at high pressures.

V. PREDICTIONS AND CONCLUSIONS

We now turn to predictions of the theory. First, we note that our model predicts reentrant behavior in the P-T phase diagram. In Fig. 4, we see that below room temperature, the LCST is lowered with *decreasing* pressure. At these temperatures and at low pressure, our model predicts fully dressed (with water) PEO chains whose solvent quality becomes poorer as one lowers temperature, thereby reducing the pressures required to initiate phase separation. The reduction in solvent quality at lower temperatures may be due to (i) van der Waals attraction between them or (ii) the establishment of the water tetrahedral network with less liable H bonds, which frustrates the fit between PEO and the water network. Reentrant behavior has indeed been observed recently in the P-T phase diagram of poly(N-vinyl-2-pyrrolidone) in water [28].

As clearly shown in Eq. (36), our theory predicts a lower critical solution pressure (LCSP) P-ϕ phase diagram that closely resembles typical LCST T-ϕ phase diagrams predicted by Flory-Huggins theory [31]. In Fig. 6, we show a plot of the spinodal and binodal pressure versus concentration with the data from a preliminary experimental study of Sun and King [44]. Our coexistence curve (i.e., binodal) appears to depend weakly on concentration in agreement with experiment [18,44]. However, more experimental data are needed to determine if the P-ϕ coexistence curve has the form of a LCSP curve as predicted in Eq. (36).

Throughout this work, we have concentrated on the regime where $\overline{m}/N\phi\ll1$ (i.e., the volume fraction of H-bonded solvents is small) and Eq. (30) is valid. We briefly discuss one consequence of complex formation between solvent and polymer displayed in the exact expression of our free energy

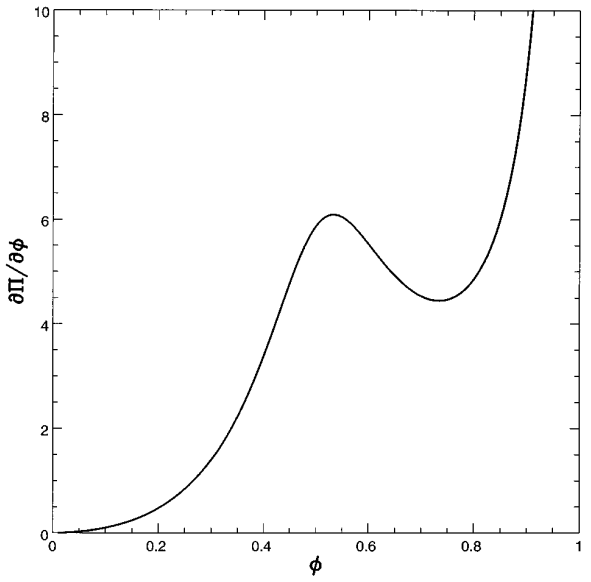

FIG. 7. Theoretical osmotic modulus $\partial\Pi/\partial\phi$ of PEO in water in units of k_BT/a^3, where a is the length of a monomer versus volume fraction of polymer ϕ, calculated for $N=1000$ at $T=275$ K.

shown in Eqs. (11) and (12) that does not appear in the standard Flory-Huggins theory. At ambient pressures and low temperatures, our free energy develops a sharp minimum as a function of concentration at $\phi\sim 0.5$. One way of observing this would be a measurement of the osmotic modulus $\partial\Pi/\partial\phi$. If a system is well described by Flory-Huggins theory (as ours is at high temperatures), the osmotic modulus is given by

$$\frac{\partial\Pi}{\partial\phi}\sim\frac{1}{N}+\frac{1}{1-\phi}-(1+2\chi\phi). \tag{37}$$

As a function of concentration, $\partial\Pi/\partial\phi$ is either monotonically increasing ($\chi\leqslant 0.5$) or exhibits a *minimum* at $\phi=1-1/\sqrt{2\chi}$ ($\chi>0.5$) and diverges as the amount of solvent approaches zero ($\phi\to 1$). In Fig. 7, we plot the osmotic modulus versus concentration calculated using Eq. (11) at $T=275$ K. In contrast to Eq. (37), the osmotic modulus develops a local *maximum* at $\phi\sim 0.5$. At such low temperatures, our system begins to resemble a polymer melt of fully dressed chains with the amount of *free solvent* approaching a small number as $\phi\to 0.5$. As we lower the temperature further, this maximum becomes a singularity as $T\to 0$, where the free solvent approaches zero as $\phi\to 0.5$, similar to the singularity encountered in the standard Flory-Huggins case as $\phi\to 1$. We note that this maximum may be obscured by PEO crystallization that occurs at weight fractions ~ 0.5.

In conclusion, we have shown that the solution theory of hydrosoluble polymers introduced by Matsuyama and Tanaka [1], where a polymer and solvent form association complexes, is well approximated by a simpler theory in which fluctuations in the number of associating solvents is neglected. In the limit of small volume fraction of associated solvents, the resulting free energy has the standard Flory-Huggins form with a good solvent contribution to the effective χ parameter, which comes from the fraction of solvents H bonded to the chain. This simple theory is capable of semiquantitatively explaining the observed T-P-ϕ phase behavior of PEO in water.

Despite the relative successes of this simple model in capturing the phase behavior of PEO in water, we have neglected effects that may be important in understanding the solution behavior of hydrosoluble polymers and PEO in particular.

(i) Cooperativity. PEO has been reported to partially retain in aqueous solution the 7_2 helix structure observed in pure crystalline form [45]. The helical structure observed in aqueous solution is attributed to H bonding between water and PEO, which is reported to display cooperativity similar to the helix-coil transition in polypeptides [45,46]. We note that the lowest order in $\mathcal{L}(T)$ approximation to m/N shown in Eq. (22) has exactly the same temperature dependence as the fraction of helical segments $\theta(T)$ in a helix-coil model with no cooperativity [46]. Incorporating cooperativity into our model is planned to be the subject of future investigations.

(ii) Saturation of the H bond. In a dense monomer environment, we expect monomer-monomer contacts to suppress H bonding between a solvent and polymer, thereby leading to a concentration-dependent χ parameter that increases with the volume fraction of polymer [20]. This may account for the discrepancy at higher concentrations between the observed and experimental T-ϕ coexistence curves shown in Fig. 3. Measurements of the effective χ parameter of PEO in water from vapor liquid equilibrium data indicate that the solvent quality indeed becomes poorer with increasing volume fraction of the polymer [14,16]. We leave this question to a future paper.

(iii) Crystallization of a polymer. As mentioned above, PEO crystallizes in water below ~ 70 °C in the weight fraction range 0.5–1 [7,16]. The specific monomer-monomer and monomer-water interactions that lead to crystallization may manifest themselves in more dilute aqueous solutions. They may account for the reported aggregation of PEO in dilute solutions below ~ 70 °C and explain the vapor-liquid equilibrium data mentioned in (ii) above. In the Appendix, we show that our model does not explain aggregate formation.

ACKNOWLEDGMENTS

We appreciate conversations with G. Fredrickson, T. Sun, H. E. King, Jr., and J. C. Selser. We especially appreciate T. Sun and H. E. King, Jr. for allowing us to present unpublished data shown in Fig. 6. This work has been supported by NSF Grant Nos. DMR-8-442490-21795 and (MRL) DMR 91-23048.

APPENDIX: AGGREGATE FORMATION

We now show that the model of hydrosoluble polymers represented by the free energy shown in Eqs. (11) and (12) does not explain aggregate formation. More specifically, there is no formal connection between our model and that of de Gennes [19]. To see this, we expand the exact free energy [Eq. (11)] in $(m/N)\phi$. We find contributions to the free energy that favor mixing between a polymer and solvent to all

orders in $(\overline{m}/N)\phi$. Therefore, we expect all virial coefficients above second order to be *positive*. More explicitly, we see from Eq. (14) that $0 \leq \mathcal{L} \leq 1$; thus, from Eqs. (18) and (19), we see that $w > 0$ and $u > 0$ for all T. With the fitting parameters that we obtain for PEO in water, $v > 0$ for T ranging from 0 °C to 70 °C.

[1] A. Matsuyama and F. Tanaka, Phys. Rev. Lett. **65**, 341 (1990).

[2] *Water-Soluble Polymers*, edited by N. B. Bikales (Plenum, New York, 1973).

[3] *Chemistry and Technology of Water-Soluble Polymers*, edited by C. A. Finch (Plenum, New York, 1973).

[4] *Water-Soluble Polymers: Recent Developments*, edited by Y. L. Meltzer (Noyes Data Corp., Park Ridge, NJ, 1979).

[5] *Encyclopedia of Polymer Science and Engineering*, 2nd ed., edited by H. F. Mark, N. B. Bikales, C. G. Overgerger, and G. Menges (Wiley, New York, 1986).

[6] *Water-Soluble Polymers for Petroleum Recovery*, edited by G. A. Stahl and D. N. Schulz (Plenum, New York, 1988).

[7] *Water-Soluble Synthetic Polymers: Properties and Uses*, edited by P. Molyneux (CRC, Boca Raton, FL, 1983).

[8] F. E. Bailey and J. V. Koleske, *Poly(ethylene oxide)* (Academic, New York, 1976).

[9] K. Devanand and J. C. Selser, Macromolecules **24**, 5943 (1991).

[10] R_g is the polymer radius of gyration and N the number of monomer units on the chain.

[11] C. S. Hudson, Z. Phys. Chem. **62**, 499 (1904).

[12] G. Jackson, Mol. Phys. **72**, 1365 (1991).

[13] S. Saeki, N. Kuwahara, M. Nakata, and M. Kaneko, Polymer **17**, 685 (1976).

[14] Y. C. Bae, J. J. Shim, D. S. Soane, and J. M. Prausnitz, J. Appl. Polym. Sci. **47**, 1193 (1993).

[15] H. L. Cox and L. H. Cretcher, J. Am. Chem. Soc. **48**, 451 (1926).

[16] G. N. Malcolm and J. S. Rowlinson, Trans. Faraday Soc. **53**, 921 (1957).

[17] R. L. Cook, H. E. King, Jr., and D. G. Peiffer, Macromolecules **25**, 2928 (1992).

[18] R. L. Cook, H. E. King, Jr., and D. G. Peiffer, Phys. Rev. Lett. **69**, 3072 (1992).

[19] P. G. de Gennes, C. R. Acad. Sci., Ser. II **313**, 1117 (1991).

[20] S. Bekiranov, R. Bruinsma, and P. Pincus, Europhys. Lett. **24**, 183 (1993).

[21] They do not, however, address the issue of the closed loops shrinking to a point.

[22] The question of whether this aggregated phase is an inherent property of the pure PEO-water system or due to impurities (in solution and/or along the backbone of the polymer chain) is a source of controversy in the experimental literature [23,24]. There have been reports of carefully prepared solutions of PEO in water that do not aggregate [25].

[23] K. Devanand and J. C. Selser, Nature **343**, 739 (1990).

[24] D. Boils and M. L. Hair, J. Colloid Interface Sci. **157**, 19 (1993).

[25] J. C. Selser (private communication).

[26] W. P. Polik and W. Burchard, Macromolecules **16**, 978 (1983).

[27] P. P. Poole, F. Sciortino, T. Grande, H. E. Stanley, and C. A. Angell, Phys. Rev. Lett. **73**, 1632 (1994).

[28] T. Sun and H. E. King, Jr. (unpublished).

[29] We show in Sec. IV that application of pressure reduces the effective number of bonding sites $f/N < 1$; thus, we will express all derived quantities explicitly in terms of f/N.

[30] S. A. Safran, *Statistical Thermodynamics of Surfaces, Interfaces, and Membranes* (Addison-Wesley, Reading, MA, 1994).

[31] P. G. de Gennes, *Scaling Concepts in Polymer Physics* (Cornell University Press, Ithaca, 1988).

[32] D. Poland and H. A. Scheraga, *Theory of Helix-Coil Transitions in Biopolymers* (Academic, New York, 1970).

[33] We note that our theory contains two energy states for a solvent, namely, that of a bound (to a polymer) solvent and an unbound solvent, where we do not explicitly take into account the water-water H-bond interaction. Clearly, inclusion of this effect would introduce three energy states for a solvent corresponding to (i) a solvent being H bonded to the polymer, (ii) a solvent being bonded to another solvent, and (iii) a solvent being unbonded. Thus $\Delta\mathcal{E}_0$ is an effective average of the following two energy differences: (i) the energy difference between a solvent H bonded to the chain and H bonded to another solvent and (ii) the energy difference between a solvent H bonded to the chain and an unbonded solvent. We plan to include the H-bonded water network in a theory of hydrosoluble polymers as the subject of future investigations.

[34] The second virial coefficient v shown in Eq. (17) is identical to that found by MT [1], indicating that fluctuations in m/N do not contribute to the free energy at the second virial level.

[35] NMR experiments of K.-J. Liu and J. L. Parsons, Macromolecules **2**, 529 (1969), on PEO in water suggest that the fraction of ''intact bonds'' does not change significantly upon increasing temperature from 30 °C to 80 °C. Rather than ''break,'' the H bond may bend, which would distort the local water network. In our theory, a bond is either completely formed or ''broken''; thus our theory would predict the number of broken bonds to be greater than the actual PEO in water system, which, in principle, exhibits bond bending.

[36] R. Kjellander and E. Florin, J. Chem. Soc. Faraday Trans. 1 **77**, 2053 (1981).

[37] J. S. Walker and C. A. Vause, Sci. Am. **256** (5), 90 (1987).

[38] MT [1], Bae *et al.* [14], and the present authors compared our calculated binodals to the cloud points, which were assumed to be a measurement of the coexistence curve rather than the spinodal. This is not obvious and requires further investigation.

[39] I. C. Sanchez, in *Polymer Compatibility and Incompatibility*, edited by K. Solc (MMI, New York, 1982), pp. 59–76.

[40] D. Patterson and A. Robard, Macromolecules **11**, 690 (1978).

[41] L. Zeman and D. Patterson, J. Phys. Chem. **76**, 1214 (1972).

[42] E. Maderek, G. V. Schulz, and B. A. Wolf, Makromol. Chem. **184**, 1303 (1983).

[43] S. Rostami and D. J. Walsh, Macromolecules **18**, 1228 (1985).

[44] T. Sun and H. E. King, Jr. (private communication).

[45] J. Maxfield and I. W. Shepherd, Polymer **16**, 505 (1975).

[46] B. H. Zimm and J. K. Bragg, J. Chem. Phys. **31**, 130 (1959).